Academic Journal of International University of Erbil

Journal Homepage: https://ojs.cihanrtv.com/index.php/public

PRINT-ISSN: 2519-6928 Online-ISSN: 3080-7174



AI-Based Classification of Mandibular Distal Root Canal Curvature: Using Deep Learning on Panoramic Radiographs

Hast Hadi Raouf 1*0, Narin Khalida Akrawi20

^{1,2} Department of Software Engineering and Informatics, College of Engineering, Salahaddin University, Erbil 44001, Kurdistan Region, IRAO

DOI: https://doi.org/10.63841/iue24519

Received 03 Jul 2025; Accepted 16 Jul 2025; Available online 25 Oct 2025

ABSTRACT:

Root canal morphology, particularly the curvature of the root canals, plays a crucial role in the efficacy of endodontic diagnosis and treatment planning. Yet, assessing this morphology typically relies on manual annotation and interpretation of dental radiographs, which can be time-consuming and prone to human error. These challenges are especially pronounced in low-resource settings such as Kurdistan, the northern part of Iraq, where access to precision imaging tools is limited. This study proposes a novel AI-based framework for classifying mandibular distal root canal curvature. Furthermore, it introduces a semi-automated annotation pipeline that integrates Schneider's method with AutoCAD, facilitating the labeling of root canal curvatures for deep learning applications.

Initially, a total number of 11,490 OPG images were gathered from public and private clinics. After undergoing rigorous preprocessing, 1,166 OPG images were selected and categorized into three classes: straight, moderate, and severe, based on Schneider's method for root canal curvature classification. Three pre-trained convolutional neural network models — ResNet-101, DenseNet-121, and EfficientNet-B0 — were fine-tuned on the collected OPGs. ResNet-101 was evaluated using a fivefold cross-validation test, while DenseNet-121 and EfficientNet-B0 were fine-tuned using a two-phase transfer learning strategy. In this approach, the initial feature extractor was first frozen, followed by fine-tuning of the whole model. To address the limited sample size, data augmentation techniques were also employed to mitigate overfitting.

Among those three models, ResNet-101 achieved the highest classification accuracy, 0.907, and an F1-score of 0.907, demonstrating superior ability to capture anatomical features. These findings underscore the effectiveness and promising role of deep learning in supporting dental diagnosis, particularly in endodontics. The proposed AI framework, combined with a semi-automated annotation approach, has the potential to improve the scalability and accessibility of root canal morphology assessment even in low-resource clinical settings.

Keywords: Deep Learning, Endodontic Diagnosis, Root Canal Curvature, Schneider's Method, Panoramic Radiographs (OPG)



1 INTRODUCTION

Accurate endodontic diagnostics are crucial for the success of root canal treatment, particularly in complex tooth anatomies such as the distal first molar[1]. The first permanent tooth to emerge, the first molar, is especially vulnerable to caries and endodontic complications due to its early emergence and long functional lifespan [2]. Precise evaluation of root canal curvature is critical for avoiding procedural errors during canal preparation, such as instrument fracture or ineffective cleaning [3][4]. Traditionally, clinicians rely on Schneider's classification method due to its simplicity and accurate procedure over all the existing curvature techniques[5], which categorizes canal curvature into three types: straight, moderate, and severe. This approach is inherently subjective and susceptible to inter-observer variability, resulting in inconsistent diagnostic outcomes [6] A key challenge addressed in this study is the limitation of such manual classification methods, which often result in diagnostic inaccuracies and procedural risks. These issues directly impact clinical decision making, particularly in the choice of instrumentation techniques, thereby compromising the quality and success of the treatment.

Existing attempts to enhance the diagnosis of root canals with conventional images and manual methods have not effectively addressed variability and diagnostic errors. Although improvements have been made in the field of digital imaging, these methods still require clinician interpretation [6]. AI-powered and deep learning-based automated systems offer a potential alternative; however, implementing these models, particularly pre-trained ones such as ResNet, EfficientNet-B0, and Vision Transformers, into dental imaging applications, including OPGs, remains an area of research [7]. Despite their potential, these models require careful adaptation to domain-specific tasks such as root canal curvature, where annotated datasets are limited and clinical variation is high.

As mentioned earlier, accurately assessing root canal curvature is essential in endodontics; however, limited research has explored the automation of Schneider's method using deep learning, particularly on panoramic radiographs in low-resource clinical settings. The application of artificial intelligence in dentistry in Kurdistan is still in its early stages of development. To our knowledge, no previous work has utilized real-world OPGs, collected locally, to implement AI-assisted classification of root canal curvature.

The objective of this work is to fill this gap by developing and evaluating CNN-based models for classifying the distal root canal curvature of mandibular first molars using OPGs.

The key contributions of this study are as follows:

- To mark root canal curvatures effectively and precisely, we developed a new semi-automated pipeline that combines Schneider's approach with AutoCAD. This pipeline helps streamline data preparation for AI-based diagnostic studies in endodontics.
- On a clinically relevant binary classification task (straight vs. moderate curvature) and excluding severe cases due to dataset limitations, we evaluate three pre-trained deep learning models: ResNet-101, DenseNet- 121, and EfficientNet-B0. This study clarifies the appropriateness of various designs for this specific application. With a macro F1-score of 0.907 on the test set, ResNet-101 is the most accurate model we found. Particularly in resource-limited environments, this shows ResNet-101's promise for endodontic diagnostic uses.
- We demonstrate the applicability of the proposed method using real-world data collected from public dental clinics in the Kurdistan region, thereby highlighting its potential to enhance access to advanced diagnostic tools in resource-constrained healthcare environments. This work demonstrates the feasibility of applying AI-assisted solutions in areas where access to specialized knowledge and tools may be limited.

2 RELATED WORKS

AI, particularly deep learning techniques such as convolutional neural networks (CNN), has shown significant results in endodontics [8]. Hiraiwa et al. [7] developed a CNN system that assessed mandibular root morphology from panoramic radiographs to determine the presence of a single or extra root, highlighting the adaptability of AI for complex anatomical structures.

However, many studies focus primarily on binary classification tasks, such as distinguishing between lesions and no lesions or tooth segmentation [9]. These approaches often overlook crucial geometric features, such as root canal curvature, which play a vital role in determining appropriate instrumentation techniques and overall treatment. Further, as they are mainly focused on lesion classification, they did not analyze curvature or morphological metrics. Roda-Casanova et al. [10]highlighted that the curvature of the canals directly influences cleaning and instrument performance.

Recent years have seen growing interest in CNN-based models for morphological classification in Endodontics. Jeon et al. [11] reported an impressive accuracy of 95.1% in predicting C-shaped canals from panoramic images, while Zhang et al. [12] validated the effectiveness of CNNs in identifying unique canal morphologies. These studies indicated that deep learning has a strong potential to capture subtle variations in canal morphology.

One major challenge in applying deep learning to dental imaging is the limited availability of high-quality labeled datasets. Transfer learning has emerged as a practical solution to overcome data scarcity. Çelik and Çelik [13]successfully employed pre-trained models, such as ResNet and YOLO, for root dilaceration detection with an accuracy of over 90%, even on small datasets. Similarly, Rashid et al. [14]used Mask-RCNN with ResNet-50 to detect caries, demonstrating high annotation agreement and software usability. While these studies validate the utility of transfer learning, they primarily focus on classifying or segmenting general features (e.g., cavities, missing teeth). They do not address domain-specific measures, such as canal curvature.

Traditional methods for evaluating root canal curvature, such as Schneider's method, remain widely used in clinical practice [6]. However, these manual assessments are prone to error and inefficiency [15] [16] Although Aung et al. [17] introduced AI-assisted detection of Schneider's angle, their work did not explore model generalization across datasets and did not utilize AI to automate Schneider's method. This article extends this line of inquiry by automating Schneider-based curvature classification.

This study builds upon prior efforts by proposing a fully automated system that applies pre-trained deep learning models, including ResNet-101, DenseNet-121, and EfficientNet-B0, to classify root canal curvature in the distal canals of first molars based on Schneider's criteria. Aiming at straight and moderate canal types (excluding severe cases due to dataset limitations), this study effectively assesses pre-trained CNN architectures that implement the training approach and compares them based on curvature classification accuracy, thereby providing architectural insights for advancing dental AI.

3 METHODOLOGY

This chapter outlines the methodology used to develop and evaluate deep learning models for classifying root canal curvature, beginning with the collection and preprocessing of OPGs gathered from multiple dental institutions in the Kurdistan region. This is followed by a comprehensive description of dataset annotation using Schneider's method, model architecture selection, training strategies, and performance evaluation metrics used in this study, as shown in Figure 16.

3.1 DATA COLLECTION AND PREPROCESSING

A total of 11,490 OPG images were collected from Kurdish patients across multiple public and private dental clinics in the Kurdistan Region. Each record includes the OPG image and the corresponding patient's age (18-40 years). Detailed data collection statistics have been presented in Figure 1. To ensure data quality, Rigorous inclusion and exclusion criteria were applied as follows:

Inclusion criteria: patients aged 18 to 40 years

Exclusion criteria: external or internal root resorption, unclear apices, previously endodontically treated teeth, primary teeth, and canals exhibiting double curvatures. After this filtering, a total of 1,166 high-quality OPG images were retained for analysis. All data collection procedures are conducted by established ethical standards and relevant privacy regulations to ensure that patient confidentiality is protected.

3.2 ANNOTATION PROTOCOL

Accurate labeling of the root canal curvature was performed using Schneider's method, a widely accepted technique for evaluating mandibular molar curvature.

3.2.1 DATASET LABELLING

We used AutoCAD software to manually plot three anatomical points[18], as shown in Figure 1. Point A is a straight line drawn on the image's axis. Point B, which is marked where the flare starts to deviate, and Point C is marked at the apical foramen. The angle formed by the intersection of these lines was measured automatically. Using the classification system from [15], we categorized the canals based on curvature: Straight: if the angle is less than 5°, Moderate: if the angle is 5 - 20°, Severe: if the angle is greater than 20°. The final dataset included 665 cases of type 1 (0-5°), 765 cases of type 2 (6-20°), and 87 cases of type 3 (larger than 20°), combining data from both sides.

To ensure accuracy, two endodontic specialists subsequently validated the labelled dataset.

3.2.2 DATASET ANNOTATION

To isolate the region of interest (ROI), we used the bounding box coordinates of the distal canal of the first molar to crop each image. We cropped all the images carefully to retain only the annotated area, minimizing background clutter and discarding unnecessary anatomical details. This preprocessing operation helped guide the model to focus on learning diagnostic features.

As shown in Figure 2, a bespoke script organized each image from a given directory and utilized OpenCV's selection feature to assist in manual ROI picking. After drawing the bounding box, an equivalent label—e.g., "Straight_Left," "St_Right," or "Moderate_Left", Moderate_Right—was labeled manually, depending on the configuration of the canals. The filename of the image, image shape, bounding box coordinates, and the assigned label were then saved in an organized CSV file for future processing.

3.3 MODEL ARCHITECTURE SELECTION

Due to time and resource limitations, our dataset was relatively small. To address this challenge, we fine-tuned three pre-trained convolutional neural networks — ResNet-101, EfficientNet-B0, and DenseNet-121 — using transfer learning. All three networks were initially pretrained on the ImageNet dataset and then adapted to our application-specific diagnostic task by further training them on our dataset.

3.3.1 RESNET-101

ResNet-101, a part of the Residual Network family presented by [19], is a deep convolutional neural network with 101 layers. It incorporates residual connections—skip connections that permit the gradients to skip one or several layers, avoiding the vanishing gradient issue typical of deep networks. The network consists of an initial convolutional block

followed by 33 residual blocks, which comprise four stages (Conv2_x to Conv5_x), resulting in a network with 44.5 million parameters.

We selected the ResNet-101 model for this study due to its depth, which supports the effective extraction of features, making it suitable for detecting slight differences in the curvature of root canal morphology.

3.3.2 EFFICIENTNET-B0

EfficientNet-B0, introduced by [20], employs a compound scaling method that uniformly scales network depth, width, and resolution using a fixed set of scaling coefficients. We utilized EfficientNet-B0, which comprises approximately 19 million parameters, a deeper yet computationally balanced architecture, and a highly optimized structure that incorporates mobile inverted bottleneck convolution (MBConv) blocks. Since it offers fast inference speeds, requires minimal memory, and remains highly accurate, we decided to utilize it as a resource-effective model, especially in the context of resource-limited regions such as Kurdistan.

3.3.3 DenseNet- 121

DenseNet-121, proposed by[21], features dense connections where each layer receives input from all previous layers. DenseNet-121 was chosen for this work because it has a compact architecture and features that propagate information quickly, and it has been successfully applied in medical imaging applications before. DenseNet-121 differs from other convolutional networks in that it utilizes dense connections, which means that each layer receives information from all the preceding layers. This structure encourages the reuse of many features and improves gradient flow. This reduces the risk of missing gradients and enables the network to function effectively with fewer parameters, approximately eight million in the case of DenseNet-121. These benefits are particularly beneficial for dental image classification tasks that involve handling small, uneven datasets.

For each model, the original classification head is replaced by:

- a dropout layer (p=0.6 for ResNet-101, p=0.5 for EfficientNet-B0 and DenseNet 121)
- a fully connected layer with two outputs (straight and moderate classes)

Figures 3-8 illustrate the original and modified architectures for each network.

3.4 TRAINING STRATEGY

To maximize model performance and minimize overfitting on the limited dataset, we implemented a two-phase transfer learning strategy, as shown in Figure 15.

Phase 1: Feature Extractor Training (Warm-up Phase)

The initial training phase focuses on adapting the newly initialized classification head to the dental imaging domain while preserving the valuable feature extraction capabilities learned from ImageNet pre-training. In this phase of transfer learning, the convolutional base of the pre-trained network was frozen, and the newly added classification head had only been trained. This method enabled the model to adjust to the task with minimal training overhead

Implementation Details for the (DenseNet-121, EfficientNet-B0, ResNet-101)

The model was trained using the Adam optimizer with a learning rate of 0.001 and utilized the Cross-Entropy Loss function. Regularization was achieved by applying a weight decay of 0.001 to mitigate overfitting. The model had already undergone training for 10 epochs, and performance on the validation set had been recorded for each epoch to retain the optimal weights.

Phase 2: Full Network Fine-tuning

The second phase enables comprehensive network adaptation through end-to-end training, allowing all network parameters to adapt to the specific requirements of canal angulation classification.

General Implementation (DenseNet-121, EfficientNet-B0):

- Duration: 20 epochs providing comprehensive fine-tuning while preventing overfitting
- Layer unfreezing: All network parameters become trainable for complete adaptation
- Learning rate: 1×10⁻⁴ ensuring stable fine-tuning without catastrophic forgetting
- Scheduler: ReduceLROnPlateau with patience=3 for adaptive learning rate adjustment
- Regularization: Weight decay of 1×10⁻³ maintaining generalization capability

Specialized Implementation (ResNet-101)

- Cross-validation integration: 5-fold cross-validation for robust performance estimation, training each fold for 20 epochs.
- Data utilization: Combined training and validation sets (85% of total data) for cross-validation
- Fold management: Fresh model instantiation for each fold ensuring unbiased evaluation
- Learning rate: 1×10⁻⁴ ensuring stable fine-tuning without catastrophic forgetting
- Scheduler: ReduceLROnPlateau with patience=3 for adaptive learning rate adjustment
- Early stopping: 7-epoch patience preventing overfitting while maximizing learning
- -Regularization: Weight decay of 1×10⁻³ maintaining generalization capability

3.5 VALIDATION AND TESTING

This section describes the methods used to evaluate the performance of the models during training, ensuring that they generalize effectively to unseen data and avoid overfitting.

3.5.1 VALIDATION STRATEGY FOR DENSENET-121, EFFICIENTNET-B0

To asses model reliability and generalizability, a robust validation strategy was implemented. The dataset was divided into three sets, with a 70:15:15 ratio used to separate the entire dataset into training, validation, and test sets. To prevent data leaking, the validation set was rigorously separated from the training and testing data and functioned as an objective reference to track model performance during both training phases. This offered a compromise between computational efficiency and steady gradient updates, particularly when a batch size of 16 was used for training, balancing gradient stability and computational efficiency.

Crucially, PyTorch's DataLoader setting (shuffle=True) was used to randomly shuffle the training data at each epoch. This randomization improved generality by preventing the model from picking up order-specific biases after each training period; the model's accuracy and validation loss were computed.

Using a ReduceLROnPlateau scheduler, these metrics were used to modify the learning rate dynamically. If validation loss did not improve for three consecutive epochs, the learning rate was reduced by a factor of 0.5. This flexible method improved convergence toward ideal weights and stabilized the training process. To avoid overfitting and conserve resources, the model weights with the highest validation accuracy were retained for final testing. Fair comparisons and accurate model selection for further assessment were guaranteed by this uniform validation pipeline across all model architectures.

3.5.2 CROSS-VALIDATION STRATEGY FOR RESNET-101

For ResNet-101, a two-phase training was used. An initial 70:15:15 split was utilized, resulting in (70% training set, 15% validation set, and 5% test set).

Phase 1 ("warm-up" final layer): The backbone was frozen, and only the newly added classification head was trained on the 70% split (with the backbone frozen, only the new head was trained). Validation was performed on the 15% validation set after each epoch to identify the best checkpoint. The test set was not used in this analysis. Full model fine-tuning was performed using five-fold cross-validation on the combined 85% (training and validation datasets). The final evaluation proceeds as follows. First, the single "best" model instance was identified based on the highest validation accuracy across the five folds.

For the final evaluation, the strictly held-out 15% test dataset was used. To ensure consistency, the same preprocessing steps, including feature scaling, normalization, and augmentation pipelines, are applied during training, particularly with a batch size of 16, maintained to optimize training efficiency and gradient stability. As in earlier phases, PyTorch's DataLoader (with shuffle=True) setting was used to randomly shuffle the training data at each epoch.

3.6 AUGMENTATION TECHNIQUES

Given the limited dataset and to improve generalization and reduce overfitting, a wide range of data augmentation techniques were used during the training phase for all three pre-trained models. To ensure consistency across batches and compliance with pre-trained model architectures, all input images across the training, validation, and test sets were scaled to a fixed resolution of 224×224 pixels.

To maintain the integrity of model evaluation, four augmentation approaches were applied just to the training dataset, leaving the validation and test sets unchanged. This was done in addition to resizing the image. Among these training-specific changes were:

• Random Rotation: To replicate variations in patient placement and the angle of picture acquisition, images were randomly rotated within a $\pm 30^{\circ}$ range.

- When used with probabilities of 0.5 and 0.2, respectively, horizontal and vertical flipping added spatial variance, helping the model avoid orientation bias.
- Color Jittering: To simulate irregularities in radiography lighting and exposure circumstances, adjustments were made to brightness, contrast, saturation, and hue.
- Random Affine Transformations: To provide anatomical and positional variation to the dataset, translation and scaling changes (within $\pm 10\%$) were applied.

All images were transformed into tensors after augmentation, and the standard ImageNet mean and standard deviation values were used to normalize them. This alignment guaranteed compatibility with the pre-trained model weights. Given the circumstances, this augmentation pipeline preserved anatomical integrity while simulating genuine variability in dental radiographs, allowing the model to extract reliable and applicable characteristics from a small dataset.

4 RESULTS AND DISCUSSION

This section presents and interprets the findings from evaluating all three deep learning models — DenseNet-121, EfficientNet-B0, and ResNet-101, to distinguish their ability to classify the two classes, namely Straight and Moderate. These results are based on standard classification metrics, including accuracy, precision, recall, F1-score, confusion matrix analysis, and precision-recall curves. A summary of their performance is shown in Table 5.

4.1 PERFORMANCE VALIDATION OF RESNET-101

ResNet-101 achieved the highest performance among the tested models on the binary classification task of detecting "Straight" and "Moderate" root canal curvature. Evaluated on an independent test set comprising 217 OPGs, the model demonstrated a test accuracy of 90.70%. This level of performance suggests that the model effectively captured the distinguishing features between the two classes, even in the presence of subtle visual variations. The class-wise performance was also well-balanced. The model was fine-tuned using 5-fold cross-validation, achieving fold-wise validation accuracies ranging from 78.19% to 82.72%. as shown in the table 6.

ResNet-101 outperformed the two other models with a test accuracy and Marco F1-score of 0.907. The confusion matrix (Figure 11) correctly classifies 95 of 101 straight and 100 of 114 Moderate cases. Only 20 misclassifications occurred, confirming robust performance. The precision-recall curve (Figure 14) demonstrates that (AP=0.97) for moderate and 0.95 for straight. The depth of the architecture, along with residual connections, enables it to learn better complex curvatures and subtle textural patterns in dental radiographs.

Clinically, ResNet-101's high recall for moderate cases (0.88) means it is suitable for clinical triage, as shown in the table 3. Moderate curvature often requires careful canal instrumentation and longer procedure times. Early identification reduces the risk of iatrogenic complications. This model shows strong potential as a real-time clinical decision support system.

4.2 PERFORMANCE VALIDATION OF EFFICIENTNET-BO

EfficientNet-B0 demonstrated moderate yet stable performance, achieving a test accuracy of 74.88%. While this is lower than ResNet-101, it still indicates a reasonable level of accuracy, particularly given its lightweight architecture.

The confusion matrix (Figure 10) shows that 71 out of 95 straight cases and 90 out of 120 moderate cases were correctly classified. Misclassifications occurred in both directions, with some Straight cases being labeled as moderate and vice versa. The PR curve (Figure 13) indicates greater confidence in predicting the Moderate cases (AP = 0.84) compared to the straight case (AP = 0.76), which aligns with its slightly better precision for moderate cases (0.79).

Despite its parameter efficiency and smaller size, EfficientNet-B0's lower recall for moderate cases (0.75), as shown in Table 4, limits its reliability when high diagnostic sensitivity is required. The shallower architecture may not fully capture subtle anatomical differences in curvature. Therefore, while this model is attractive for its resource-limited environment, it must be used with caution in clinical settings where sensitivity to complex root morphology is crucial.

4.3 PERFORMANCE VALIDATION OF DENSENET-121

DenseNet-121 demonstrated strong generalization capability with a test accuracy of 80.0%. The confusion matrix (Figure 9) revealed that 91 out of 101 straight cases were correctly classified, while 81 out of 114 moderate cases were also accurately detected. However, 33 moderate canals were misclassified as straight, showing some confusion when curvature is close to the borderline threshold.

The model's PR curves (Figure 12) confirm stronger separation for the Moderate class (AP = 0.90) compared to the straight class (AP = 0.85), suggesting it has higher confidence in detecting moderate cases. Its dense connectivity helped retain detailed spatial features, which contributed to robust pattern recognition even in imbalanced classes.

From a clinical perspective, the model's high recall for straight class (0.90) in Table 2 is valuable in ruling out complex curvatures, ensuring that patients with simpler cases are quickly triaged. However, missing 29% of moderate canals risks understanding curvature, potentially leading to poor cleaning or instrument fracture. The model may still be helpful as a support tool, but it requires human validation in borderline cases.

CONCLUSION

This work presents a practical implementation of an AI-based system for classifying root canal curvature using panoramic radiographs, contributing to the advancement of diagnostic support tools in endodontics. It further introduces a semi-automated annotation pipeline that integrates Schneider's technique with AutoCAD to support more efficient dataset preparation in endodontics. While the actual reduction in time and complexity has not been measured, the method provides a framework that may help streamline manual annotation tasks.

Among the evaluated models, ResNet-101, DenseNet-121, and EfficientNet-B0, ResNet-101 proved to be the most accurate and robust model, with a macro F1-score of 0.907. These results highlight the diagnostic potential of pre-trained convolutional neural networks in dental imaging, particularly in low-resource settings where advanced imaging capabilities are often limited.

The use of real-world data from public and private clinics in the Kurdistan region of Iraq further underscores the practical relevance of the proposed method. By leveraging deep learning techniques, including transfer learning, this study illustrates how effective diagnostic systems can be developed even under limited computational or imaging resources, offering a viable pathway towards accessible AI-assisted endodontic diagnosis.

FUTURE WORK

Future work should focus on expanding the dataset to include a broader range of anatomical variations, particularly cases with complex root canal configurations, such as severe curvatures, to further improve the models' generalization. Further studies are also needed, with a focus on prospective clinical validation, to test these models in actual clinical workflows and ensure their robustness, clinical accuracy, and suitability for integration into routine endodontic diagnosis.

ACKNOWLEDGEMENT

The authors wish to extend their sincere gratitude to the administrations and clinical teams at the Radiology Department of Hawler Medical University College of Dentistry, Smart Center for Oral & Maxillofacial Radiology, as well as La Denta Dental Center for granting access to their orthopantomograms used in this study. We are also grateful to our colleagues at the Department of Software and Informatics Engineering at Salahaddin University for their invaluable technical support. A special note of thanks goes to Prof. Dr. Bassam Karem Amin and Dr. Saya Hadi Raouf of Hawler Medical University College of Dentistry for meticulously validating all Schneider-based annotations and offering their expert endodontic insights, which were critical to the accuracy and clinical relevance of our work.

7. CONFLICTS OF INTEREST

The author declares no conflict of interest.

8. REFERENCES

- [1] R. Fuentes, C. Farfán, N. Astete, P. Navarro, and A. Arias, "Distal root curvatures in mandibular molars: Analysis using digital panoramic X-rays," *Folia Morphologica (Poland)*, vol. 77, no. 1, pp. 131–137, 2018, doi: 10.5603/FM.a2017.0066.
- [2] F. J. Vertucci, "Root canal anatomy of the human permanent teeth," *Oral Surgery, Oral Medicine, Oral Pathology*, vol. 58, no. 5, pp. 589–599, 1984, doi: 10.1016/0030-4220(84)90085-9.
- [3] S. W. Schneider, "A comparison of canal preparations in straight and curved root canals," *Oral Surgery, Oral Medicine, Oral Pathology*, vol. 32, no. 2, pp. 271–275, 1971, doi: 10.1016/0030-4220(71)90230-1.
- [4] C. Lucena, E. M. Souza, G. C. Voinea, R. Pulgar, M. J. Valderrama, and G. De-Deus, "A quality assessment of randomized controlled trial reports in endodontics," *Int Endod J*, vol. 50, no. 3, pp. 237–250, 2017, doi: 10.1111/iej.12626.
- [5] M. H. Malur and A. Chandra, "Curvature height and distance of MB canal of mandibular molar with Schneider angle and its comparison with canal access angle," *J Oral Biol Craniofac Res*, vol. 8, no. 3, pp. 212–216, 2018, doi: 10.1016/j.jobcr.2017.07.002.
- [6] P. Balani, F. Niazi, and H. Rashid, "A brief review of the methods used to determine the curvature of root canals," *Journal of Restorative Dentistry*, vol. 3, no. 3, p. 57, 2015, doi: 10.4103/2321-4619.168733.
- [7] T. Hiraiwa *et al.*, "A deep-learning artificial intelligence system for assessment of root morphology of the mandibular first molar on panoramic radiography," *Dentomaxillofacial Radiology*, vol. 48, no. 3, pp. 1–7, 2019, doi: 10.1259/dmfr.20180218.
- [8] S. Asgary, "Artificial Intelligence in Endodontics: A Scoping Review," *Iran Endod J*, vol. 19, no. 2, pp. 85–98, 2024, doi: 10.22037/iej.v19i2.44842.

- [9] E. G. Ha, K. J. Jeon, H. Choi, C. Lee, Y. J. Choi, and S. S. Han, "Automatic diagnosis of retention pseudocyst in the maxillary sinus on panoramic radiographs using a convolutional neural network algorithm," *Sci Rep*, vol. 13, no. 1, pp. 1–7, 2023, doi: 10.1038/s41598-023-29890-5.
- [10] V. Roda-Casanova, A. Pérez-González, Á. Zubizarreta-Macho, and V. Faus-Matoses, "Fatigue analysis of NiTi rotary endodontic files through finite element simulation: Effect of root canal geometry on fatigue life," *J Clin Med*, vol. 10, no. 23, 2021, doi: 10.3390/jcm10235692.
- [11] S. J. Jeon *et al.*, "Deep-learning for predicting C-shaped canals in mandibular second molars on panoramic radiographs," *Dentomaxillofacial Radiology*, vol. 50, no. 5, pp. 1–6, 2021, doi: 10.1259/dmfr.20200513.
- [12] L. Zhang *et al.*, "A lightweight convolutional neural network model with receptive field block for C-shaped root canal detection in mandibular second molars," *Sci Rep*, vol. 12, no. 1, pp. 1–11, 2022, doi: 10.1038/s41598-022-20411-4.
- [13] B. Çelik and M. E. Çelik, "Root Dilaceration Using Deep Learning: A Diagnostic Approach," *Applied Sciences (Switzerland)*, vol. 13, no. 14, 2023, doi: 10.3390/app13148260.
- [14] U. Rashid *et al.*, "A hybrid mask RCNN-based tool to localize dental cavities from real-time mixed photographic images," *PeerJ Comput Sci*, vol. 8, pp. 1–24, 2022, doi: 10.7717/PEERJ-CS.888.
- [15] R. C. Hartmann, M. Fensterseifer, O. A. Peters, J. A. P. de Figueiredo, M. S. Gomes, and G. Rossi-Fedele, "Methods for measurement of root canal curvature: a systematic and critical review," *Int Endod J*, vol. 52, no. 2, pp. 169–180, 2019, doi: 10.1111/iej.12996.
- [16] A. K. Navas, J.M., Doranala, S., Khushnud, A., Sinha, J., Jadhav, A.A., Gudapati, S. and Syed, "Methodology Used in the Study," *J Pharm Bioallied Sci*, 2022, doi: 10.4103/jpbs.jpbs_714_21.
- [17] M. T. Z. Aung *et al.*, "Deep learning-based automatic segmentation of the mandibular canal on panoramic radiographs: A multi-device study," *Imaging Sci Dent*, vol. 54, no. 1, pp. 81–91, 2024, doi: 10.5624/isd.20230245.
- [18] H. Nekkanti, S. Enuganti, J. S. S. Avula, P. Kakarla, S. K. Siva, and D. N. Gavarraju, "Assessment of Biomechanical Preparation Influence on Various Root Canal Curvatures," *Int J Clin Pediatr Dent*, vol. 17, no. 2, pp. 10–15, 2024, doi: 10.5005/jp-journals-10005-2760.
- [19] K. He, X. Zhang, S. Ren, and J. Sun, "Deep residual learning for image recognition," *Proceedings of the IEEE Computer Society Conference on Computer Vision and Pattern Recognition*, vol. 2016-Decem, pp. 770–778, 2016, doi: 10.1109/CVPR.2016.90.
- [20] M. Tan and Q. V. Le, "EfficientNet: Rethinking model scaling for convolutional neural networks," *36th International Conference on Machine Learning, ICML 2019*, vol. 2019-June, pp. 10691–10700, 2019.
- [21] G. Huang, Z. Liu, G. Pleiss, L. Van Der Maaten, and K. Q. Weinberger, "Convolutional Networks with Dense Connectivity," *IEEE Trans Pattern Anal Mach Intell*, vol. 44, no. 12, pp. 8704–8716, 2022, doi: 10.1109/TPAMI.2019.2918284.
- [22] A. Khan *et al.*, "Human gait recognition using deep learning and improved ant colony optimization," *Computers, Materials and Continua*, vol. 70, no. 2, pp. 2113–2130, 2022, doi: 10.32604/cmc.2022.018270.
- [23] A. Hussain, S. Ul Amin, M. Fayaz, and S. Seo, "An Efficient and Robust Hand Gesture Recognition System of Sign Language Employing Finetuned Inception-V3 and Efficientnet-B0 Network," *Computer Systems Science and Engineering*, vol. 46, no. 3, pp. 3509–3525, 2023, doi: 10.32604/csse.2023.037258.
- [24] R. Chetan, D. V Ashoka, and A. Prakash, "HybridTransferNet: Advancing Soil Image Classification through Comprehensive Evaluation of Hybrid Transfer Learning HybridTransferNet: Advancing Soil Image Classification through Comprehensive Evaluation of Hybrid Transfer Learning," 2023, [Online]. Available: https://doi.org/10.21203/rs.3.rs-3032907/v1

APPENDIX

Table 1. Number of OPG Images

Data Source	Number of OPG Images
Howler Medical University College of Dentistry	4,426
First Clinic	550
Second Clinic	2,231
Third Clinic	751
Total	7,958

Table 2. DenseNet-121 classification report

Class	Precision	Recall	F1 Score	Support
Straight	0.73	0.90	0.81	101
Moderate	0.89	0.71	0.79	114

Table 3. ResNet-101 classification report

Class	Precision	Recall	F1 Score	Support
Straight	0.87	0.94	0.90	101
Moderate	0.94	0.88	0.91	114

Table 4. EfficientNet-B0 classification report

Class	Precision	Recall	F1 Score	Support
Straight	0.70	0.75	0.72	95
Moderate	0.79	0.75	0.77	120

Table 5. Fine-tuned model performance comparison

Model	Fine-tuned	Test Accuracy	Macro Precision	Macro Recall	Macro F1
	Accuracy				
ResNet-101	82.72%	90.70%	0.907	0.909	0.907
DenseNet- 121	79.91%	80.00%	0.812	0.806	0.800
EfficientNet-B0	76.64%	74.88%	0.746	0.749	0.747

Table 6. Cross validation results for ResNet-101 training and validation accuracy across five folds

The number fold	Train accuracy	Validation accuracy
Fold 1	83.49%	82.72%
Fold 2	82.77%	78.19%
Fold 3	82.89%	80.58%
Fold 4	80.82%	79.34%
Fold 5	77.32%	78.51%

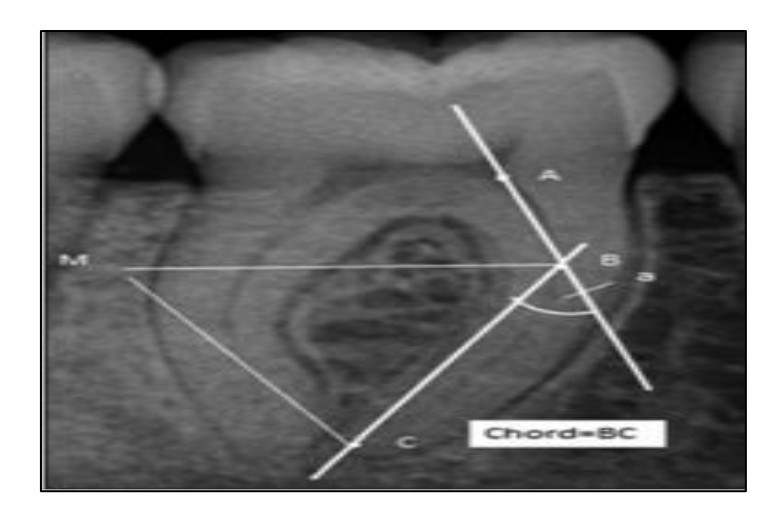


FIGURE 1. Schneider's method for measuring root canal curvature [6]

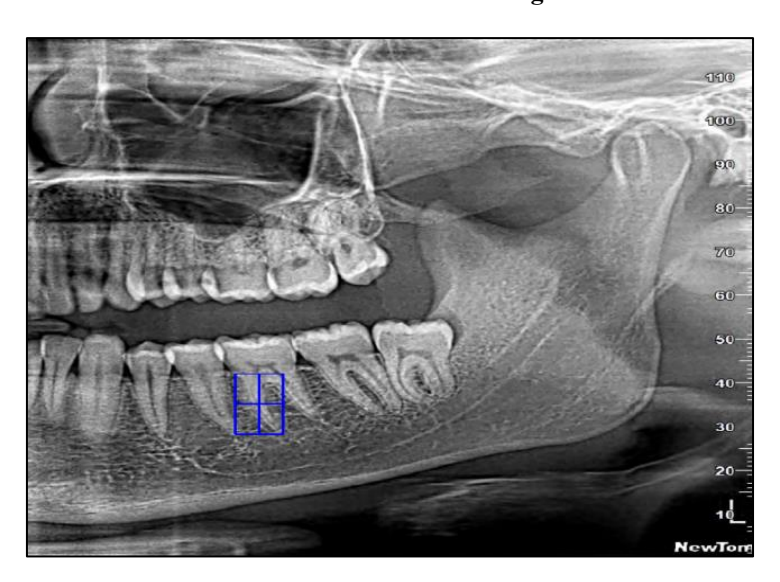


FIGURE 2. Annotation process of orthopantomogram (OPGs)

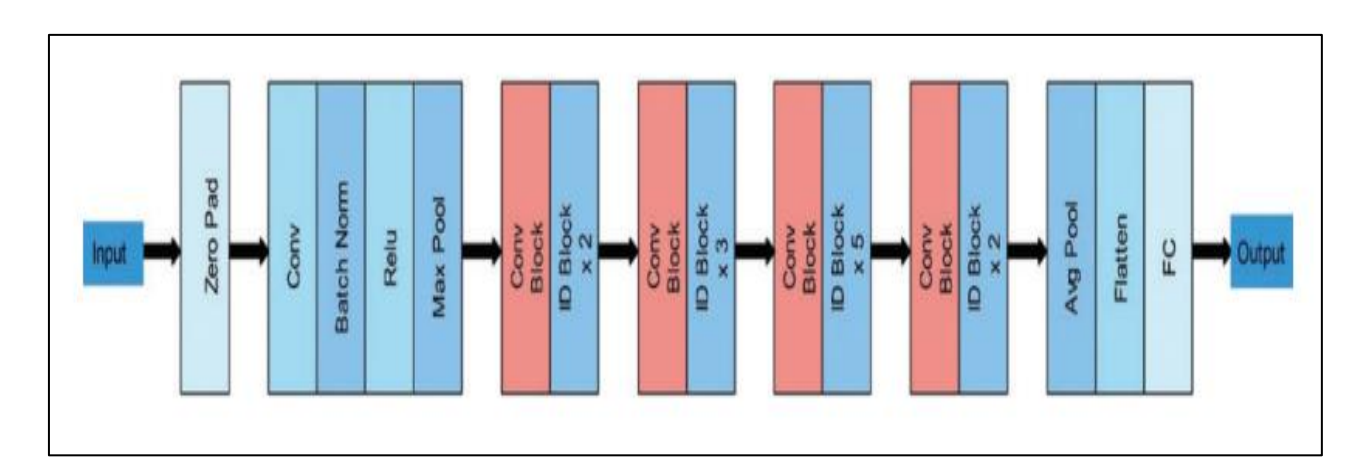


FIGURE 3. Architecture of ResNet-101 by [22]

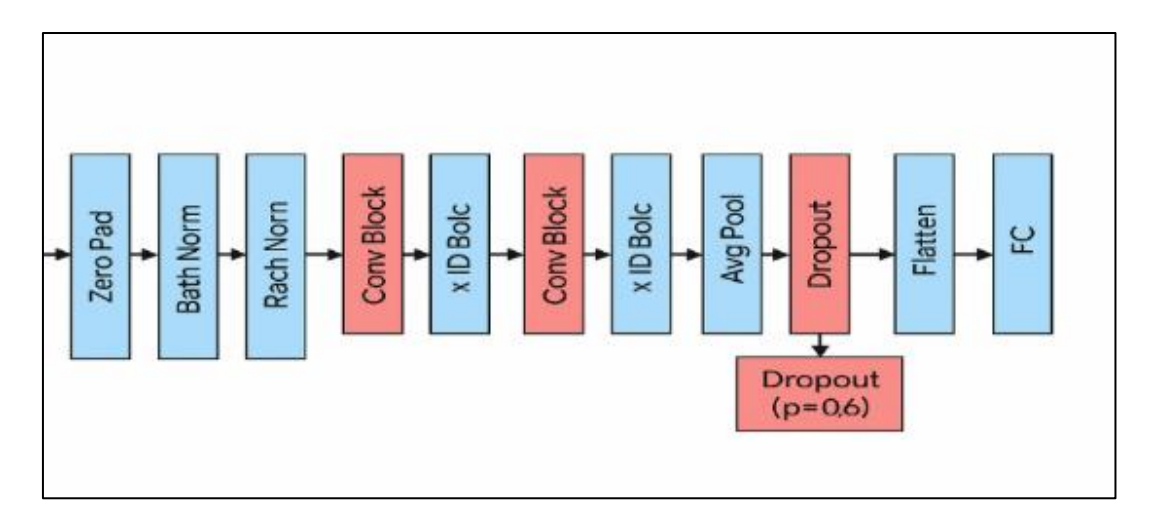


FIGURE 4. Architecture of ResNet-101 after fine-tuning for the classification task

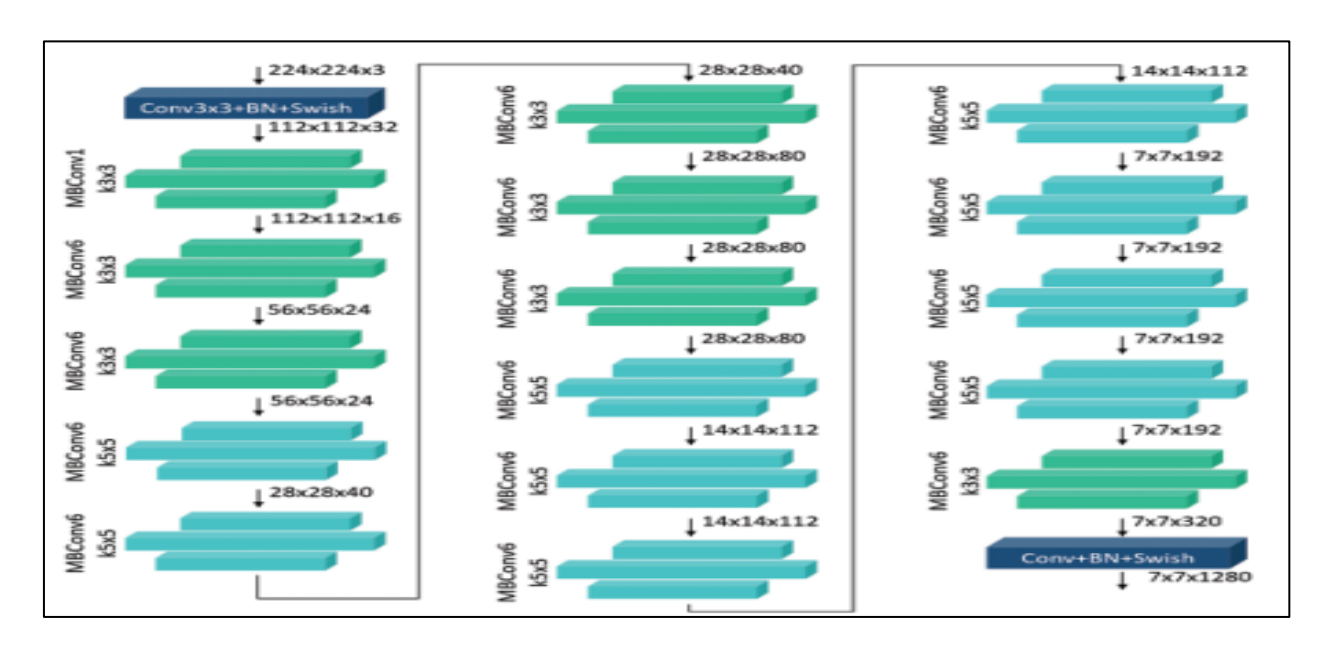


FIGURE 5. Architecture of EfficientNet-B0 by [23]

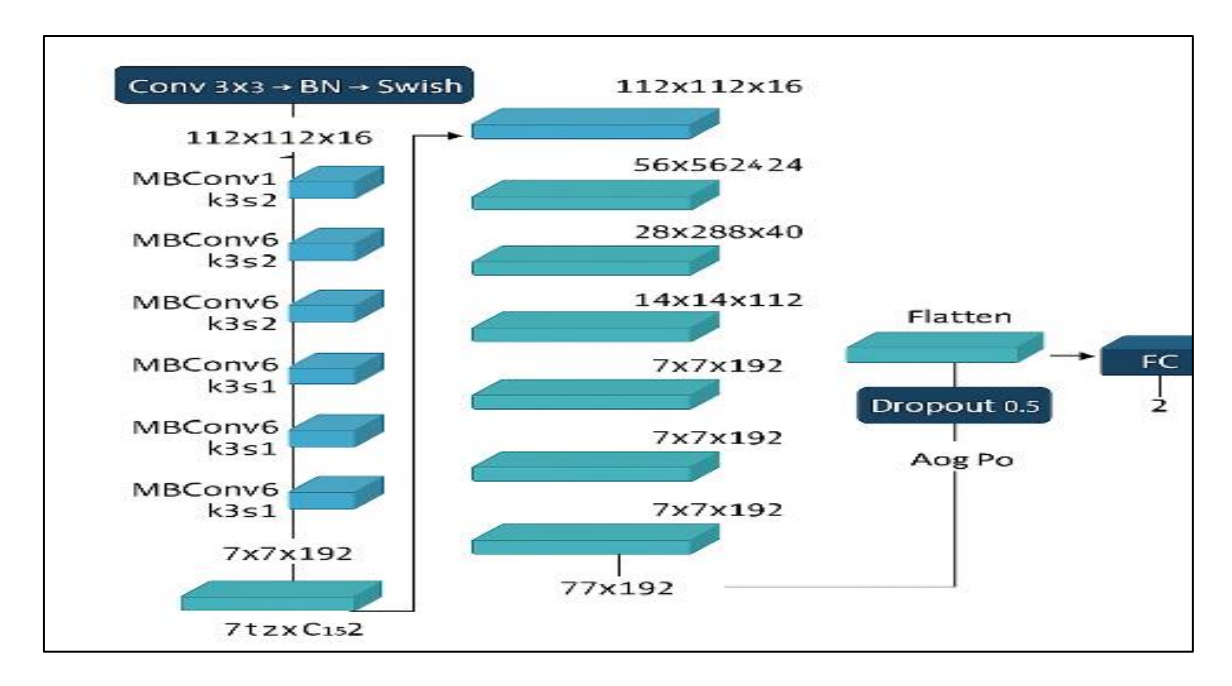


FIGURE 6. Fine-tuned ResNet-101 architecture adapted for dental root canal curvature classification

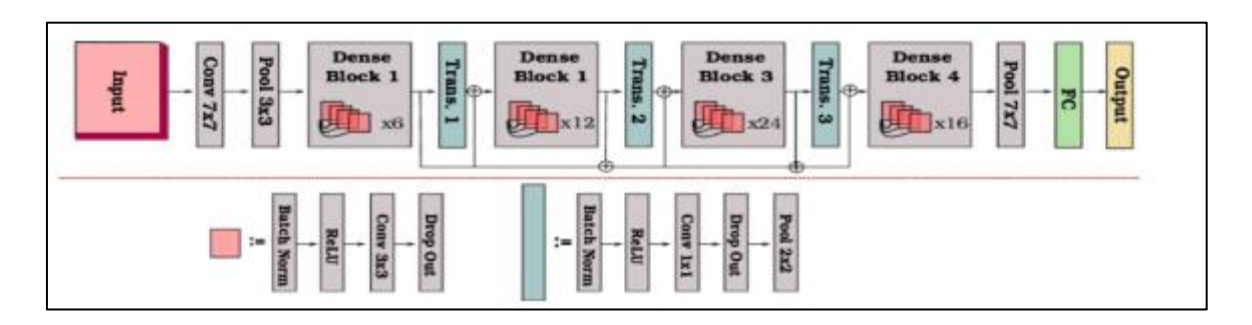


FIGURE 7. Architecture DenseNet-121 by [24]

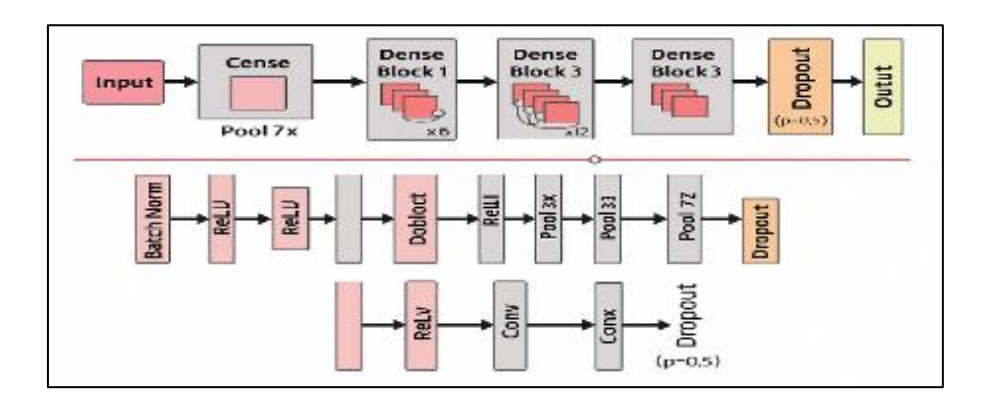


FIGURE 8. Architecture of DenseNet-121 after fine-tuning for root canal curvature classification task

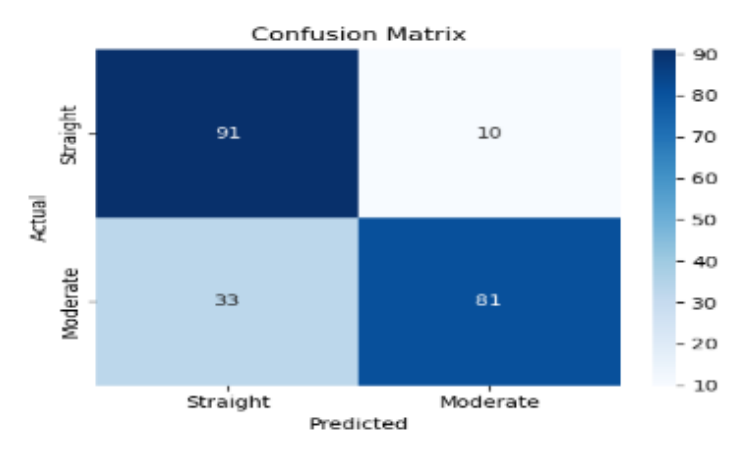


FIGURE 9. Confusion Matrix DenseNet-121 on the test dataset

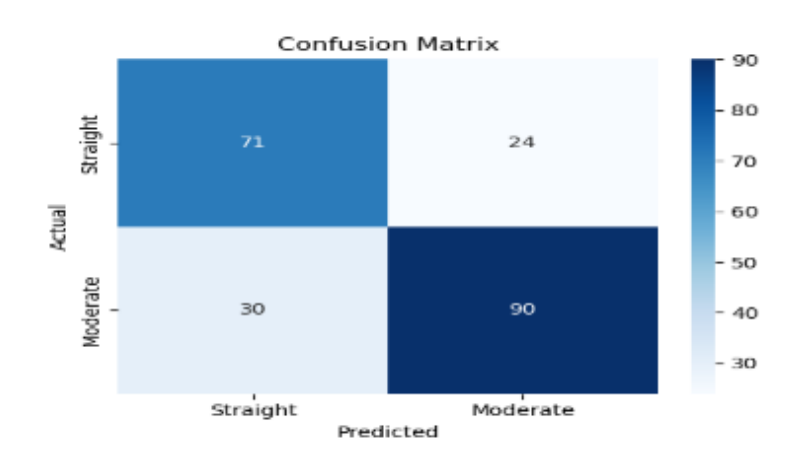


FIGURE 10. Confusion Matrix of EfficientNet-B0 on the test dataset

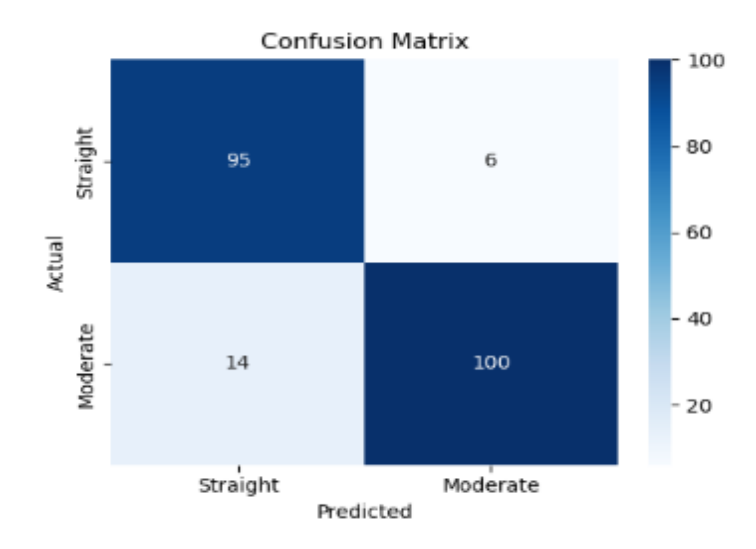


FIGURE 11. Confusion matrix ResNet-101on the test dataset

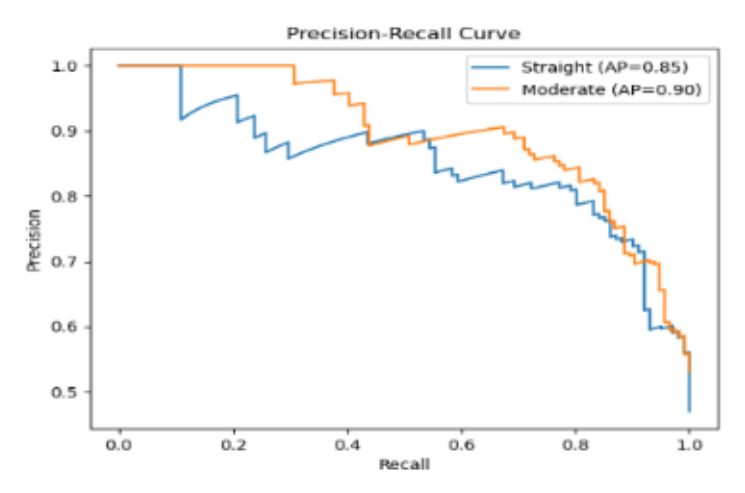


FIGURE 12. Precision and recall curve of the DenseNet-121 model

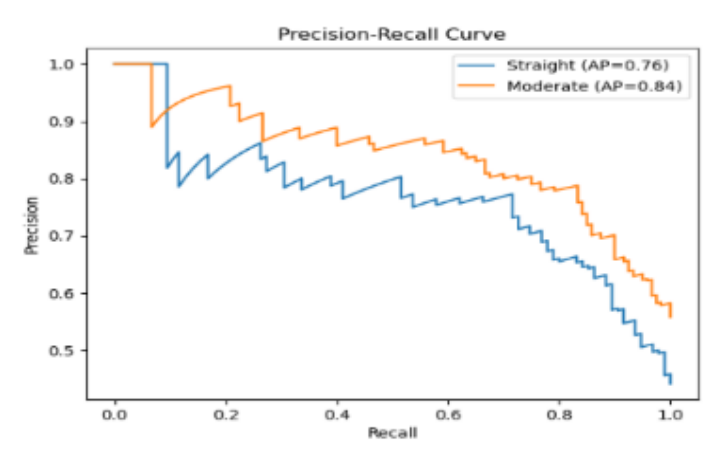


FIGURE 13. Precision and recall curve of the EfficientNet-B0 model

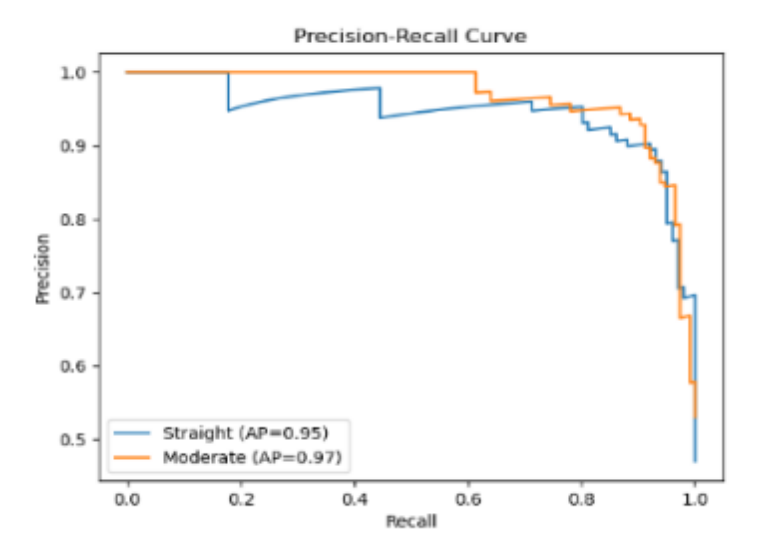


FIGURE 14. Precision and recall curve of the ResNet-101 model

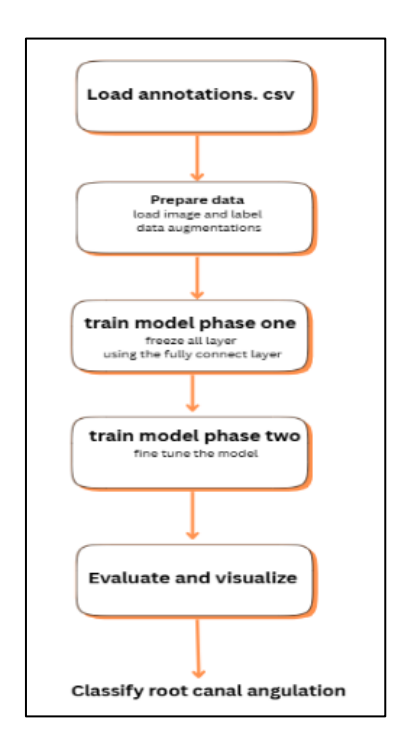


FIGURE 15. Overview of the two-phase transfer learning strategy in this study

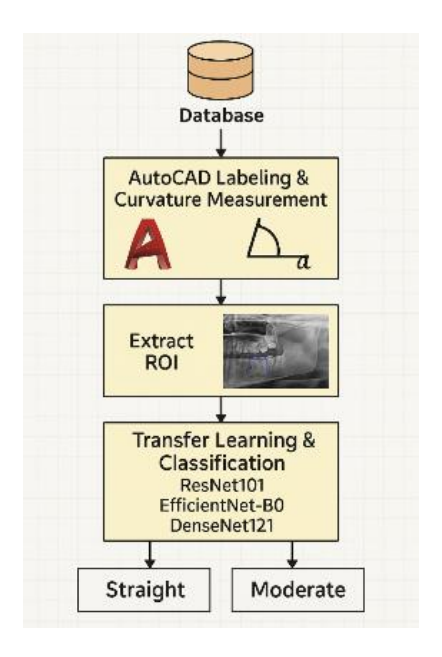


FIGURE 16. Overview of the proposed method for classifying the first molar distal canal